Cement & Concrete Composites 32 (2010) 194–203

Contents lists available at ScienceDirect

Cement & Concrete Composites

journal homepage: www.elsevier.com/locate/cemconcomp

Bond analysis of corroded reinforced concrete beams under monotonic and fatigue loads

Rania Al-Hammoud, Khaled Soudki *, Timothy H. Topper

Department of Civil Engineering, University of Waterloo, Waterloo, ON, Canada N2L 3G1

ARTICLE INFO

Article history:
Received 22 June 2009
Received in revised form 2 December 2009
Accepted 4 December 2009
Available online 25 January 2010

Keywords:
Corrosion
FRP sheets
Fatigue bond strength
Slip
Bond stress
Shear stress

ABSTRACT

This study investigated the fatigue bond behaviour of corroded steel reinforced concrete beams. Nine beams (152 × 254 × 2000 mm [6 × 10 × 78.74 in.]) were constructed and tested. Bond failure occurred in all the beams. The variables in this test series were: the type of load applied (monotonic or repeated loading), the repeated load range, whether the reinforcement inside the beam was corroded or not, and whether a carbon fibre reinforced polymer (CFRP) repair method was used or not. The fatigue life of the beams varied linearly with the range of applied load with a very shallow slope. Corroding the beams to a low corrosion level decreased the fatigue bond strength by about 30%. Corrosion caused the concrete in between the lugs of the reinforcing bars to be partially crushed due to the formation of the rust products from the corrosion process. This reduced the strength of the concrete keys and increased the rate of slip in the bar under repeated loading.

1. Introduction and background

Corrosion of steel reinforcement severely decreases the service life of reinforced concrete structures. Corrosion of reinforcing steel produces corrosion products with higher volume than the original steel resulting in cracking of the concrete surrounding the bars. Corrosion leads to a reduction in the cross-sectional area of the reinforcing steel (or mass loss) and a loss of bond between the reinforcing steel and the concrete. In service the maximum section loss in terms of reinforcing steel diameter is about 50 μm/yr. Broomfield [1] states that "less than 100 μm of steel section loss is needed to start cracking and spalling of the concrete". This means that corrosion often damages the bond between the steel and the concrete long before the reduction of the cross-sectional area of the bars becomes critical. In fact, the deterioration of bond is often critical for the serviceability performance (deflection and cracking) of reinforced concrete structures [2]. Repairing the resulting corrosion deteriorated structures is costly. According to [3], rehabilitation of reinforced concrete structures consumes more than 50% of every dollar spent on construction.

Bond is the mechanism by which stresses are transferred between the reinforcing steel bars and the concrete in a reinforced concrete member. Bond in reinforced concrete structures is made up of three components: a chemical adhesion between the concrete and the steel, friction due to the presence of small irregularities on the bar's surface, and mechanical interaction between the ribs of deformed bars and the surrounding concrete [4]. The primary bond mechanism restraining the relative slip between a deformed bar and the surrounding concrete is the transfer of forces between the bar ribs and the concrete. If the depth of concrete cover on the ribs or the spacing between the anchored bars is small, then the radial pressure which is the vertical component of the bond force will cause splitting failure. If the cover and spacing between the bars is great enough or if sufficient transverse reinforcement is provided, a splitting failure cannot develop and a pullout failure will occur or the bar will yield. In a pullout failure, the concrete between the bar lugs is sheared off from the surrounding concrete. The bond strength in a pullout failure is dependent on the strength of concrete in direct shear.

Experimental studies reported in the literature on the effect of corrosion on the bond behaviour of reinforced concrete beams under monotonic loading showed that at a low corrosion rate (about 0.04 mA/cm^2) the bond strength initially increased as corrosion progressed so long as the section was not cracked [5]. This increase was attributed to the fact that the corrosion rust products produced before cracking caused a rough surface around the bar hence increasing the friction force on the interface between the reinforcing steel and the concrete [5]. Once the concrete cracks due to corrosion, the bond stresses between the reinforcing steel and the concrete decreased and the slip of the reinforcing bar relative to the concrete sharply increased ([5–13]). This decrease in the bond strength was attributed to a decrease in the interlock between the ribs and the concrete due to a severe deterioration of the ribs; the

* Corresponding author.
E-mail address: soudki@uwaterloo.ca (K. Soudki).

0958-9465/$ - see front matter © 2009 Elsevier Ltd. All rights reserved.
doi:10.1016/j.cemconcomp.2009.12.001

increase in the width of the longitudinal cracks that reduced the concrete confinement; and the large amount of rust flakes around the bar that lubricated it and hence decreased the friction force between the reinforcing steel and the concrete [5].

Structures such as bridges and marine structures are prone to corrosion. These structures are usually subjected to repeated loading. As the live load to dead load ratio has increased (e.g. heavier trucks on bridges), the effect of repeated loading has started to govern the design for the serviceability limit state [14]. Repeated loading can initiate cracks in the concrete surrounding the steel bars that propagate as the number of load cycles increases leading to the destruction of the concrete–steel interface and slip of the steel bars inside the concrete. Repeated loading often causes serious damage to a structure under service loads that are far below the ultimate loads [15,16].

Many researchers have studied the effect of corrosion on the flexural behaviour of reinforced concrete beams [17,18]. Very few researchers have studied the effect of corrosion on the bond behaviour between the reinforcing steel and the concrete. In the research reported on bond, most investigators used pullout specimens, which do not correctly model true bond behaviour nor result in bond stress values that can be used to assess the bond behaviour in a reinforced concrete (RC) structures [5]. Also, very few experiments have been carried out to study the effect of repeated loading on the concrete–steel interface [4].

The bond between reinforcing steel and concrete is an important parameter in determining the fatigue strength and the serviceability conditions of a flexural reinforced concrete member. This research investigated the fatigue bond behaviour of corroded and uncorroded steel reinforced concrete beams under repeated loading, and examined the effect on fatigue bond strength of Carbon FRP strengthened reinforced concrete beams. Fibre reinforced polymer (FRP) reinforcement, with their ease of installation, high strength to weight ratio, high fatigue resistance and the fact that they do not corrode, have emerged as an alternative to traditional methods for the repair and strengthening of concrete structures [19].

2. Experimental program

The experimental program consisted of testing nine steel reinforced concrete beams. The nine beams were divided into three groups. Group 1 consisted of three beams tested monotonically to failure, one control (uncorroded and unstrengthened), one corroded but unstrengthened and one uncorroded strengthened beam. Group 2 consisted of three uncorroded beams tested at three different fatigue load ranges. Group 3 consisted of three corroded beams tested at three different fatigue load ranges. The beams all were of the same size with a rectangular cross-section (254 × 152 mm [10 × 6 in.]) and a length of 2000 mm (78.74 in.). Each beam was reinforced with two 20 M (19.5 mm [0.77 in.] in diameter) Grade 400 steel deformed bars as tension reinforcement. Two 8 mm (0.31 in.) smooth bars were used as compression steel reinforcement and 8 mm (0.31 in.) stirrups were used as shear reinforcement. A hollow 8 mm diameter stainless steel bar, Grade 304, was placed at a distance of 80 mm (3.15 in.) from the bottom of the beam. This steel bar was used as a cathode in the accelerated corrosion process. The stainless steel bar and the two 20 M deformed bars were extended 150 mm (5.9 in.) from one end of the beam to provide for the electrical connections necessary for accelerated corrosion. The 20 M deformed bars were bent at one end of the beam to form a standard hook and ensure that bond failure would occur at the other instrumented end of the beam. A longitudinal and a cross-sectional detail of the beams is shown in Fig. 1. In order to provide the required anchorage length of 200 mm, a low density polyethylene (LDP) tube was placed over the reinforcing bar to create un-bonded zones, in the middle and at 175 mm (6.89 in.) from each end of the beams. Also, two pockets (152 × 75 × 50 mm [5.98 × 2.95 × 1.97 in.]) at the end of the specified length were provided to allow for easy instrumentation of the tension steel.

Salted concrete formed by adding salted water (2.15% of chloride (Cl^-) by weight of cement) was placed in the anchorage zone of the beam (300 mm [11.81 in.] long and 100 mm [3.94 in.] from the bottom of the beam) to accelerate corrosion of the two 20 M deformed bars in the anchorage zone. Unsalted concrete was placed in the rest of the beam. The 28-day compressive strength of the unsalted concrete was on average 48.6 ± 4.86 MPa (7048 ± 705 psi), and for the salted concrete was on average 35.9 ± 1.34 MPa (5207 ± 194 psi).

In order to accelerate the corrosion process, the beams were subjected to a constant current density of 150 μA/cm^2 (967.74 μA/in^2) using power supplies as recommended by [20]. To ensure a constant current in the beams, the tension steel reinforcement bars of the beams were connected in series and the direction of the current was adjusted so that the tension steel served as the anode and the stainless steel bar served as the cathode. During corrosion, the beams were placed in a special chamber maintaining a mixture of moisture and oxygen. The corrosion time to achieve the desired corrosion level was estimated using Faraday's law. The corrosion resulted in an actual mass loss on average between 3.5% and 3.9%. The actual corrosion level of the steel reinforcement was determined using the mass loss analysis described in [21].

The beams were reinforced in the flexural zone with two external CFRP (each 100 mm wide × 1370 mm long [2 × 3.94 × 53.94 in.] trapezoidal in shape) sheets along both sides in order to reduce the stresses in the internal steel bars. The sheets were located with their centroid at a depth of 144 mm (5.67 in.) from the top of the beam. These CFRP sheets were tapered so that as the moment increases the curvature and the stress in the reinforcing bars

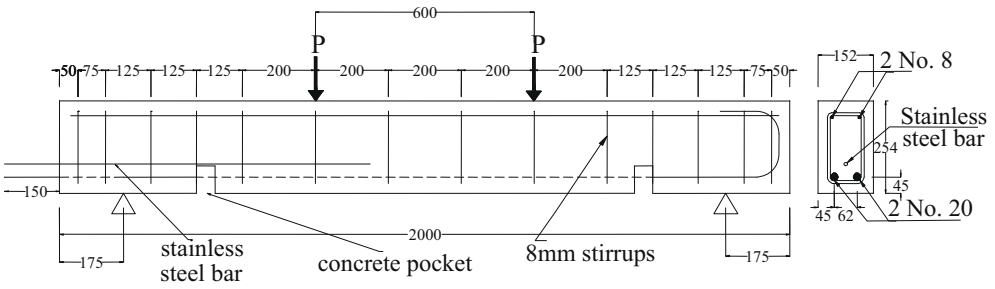

Fig. 1. Longitudinal and cross-sectional details for the beams in phase 1 (all dimensions are in mm). The hashed part of the steel reinforcement represents the un-bonded length.

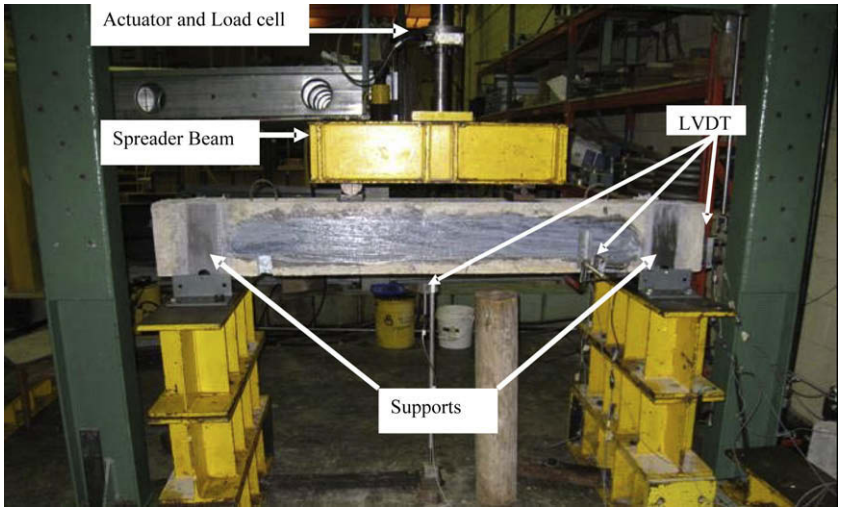

Fig. 2. Test setup.

remain constant. The taper prevents the introduction of a stress raiser at the point at which the sheet begins. The development length of the CFRP sheet was calculated to be 60 mm based on [22].

The CFRP system used was manufactured by SIKA Inc. The CFRP sheets were SikaWrap 230C and the epoxy resin was Sikadur Hex 330. The mechanical properties of the cured CFRP system are as follows: ultimate strength (715 MPa [103.7 ksi]), modulus of elasticity (61,012 MPa [8849 ksi]), elongation at break (1.09%) and thickness (0.381 mm [0.015 in.]). The CFRP sheets were applied according to the manufacturer's recommendations.

The beam end supports consisted of two L-shaped steel plates glued to the side faces of the beam at the support point (Fig. 2). The supports were glued to the beam using SIKADUR 30 and a layer of corrugated rubber such that the L-shaped plate does not touch the beam soffit at the support point. This helps eliminate the confinement effect on the bond of the steel reinforcement in concrete that would result if the supports were in direct contact with the beam.

Linear variable differential transducers (LVDTs) with an accuracy of 0.01 mm (0.0004 in.) were used to measure the slip between the steel bar and the concrete (from the loaded end and the free end) as well as the beam deflection at midspan.

Electrical resistance strain gauges (gauge length of 5 mm (0.197 in.) and 30 mm (1.18 in.) manufactured by Tokyo Sokki Kenkyujo Co., Japan were used. The 5 mm (0.197 in.) long strain gauges were placed on the steel bar in the pocket, and inside the steel bar

Table 1
Results of the current study and the results by Rteil (2007).

Research	Beam notation	Corrosion level	Load			Life to failure (cycles)
			Min. (kN)	Max. (kN)	Range (kN)	
Current study	F-U-40-n[a]	No corrosion, 0%	10	50	40	1,000,000[b]
	F-U-48-n[a]			58	48	1,000,000[b]
	F-U-55-n[a]			65	55	1,000,000[b]
	F-U-63-n[a]			73	63	1,000,000[b]
	F-U-66-n[a]			76	66	365,153
	F-U-70-n1[a]			80	70	4022
	F-U-70-n2			80	70	6524
	F-U-40-l[c]	Low corrosion, ~3.9%	10	50	40	1,000,000[b]
	F-U-41.5-l[c]			51.5	41.5	1,000,000[b]
	F-U-42.5-l[c]			52.5	42.5	1,000,000[b]
	F-U-43-l[c]			53	43	1000,000[b]
	F-U-43-l			53	43	31,662
	F-U-44-l[c]			54	44	1,000,000[b]
	F-U-45-l[c]			55	45	343,586
	F-U-46-l			56	46	2518
Rteil 2007 [23]	F45-N-T0	No corrosion, 0%	10	55	45	442,134
	F47-N-T0			57	47	31,423
	F50-N-T0			60	50	2041
	F53-N-T0			63	53	25,052
	F55-N-T0			65	55	1714
	F37-N-T5	Low corrosion, ~5%	10	47	37	2912
	F40-N-T5			50	40	222,263
	F45-N-T5			55	45	245,318
	F50-N-T5			60	50	0.5
	F55-N-T5			65	55	340

[a] One beam tested at maximum load of 50, 58, 65, 73, and 80 kN.
[b] Those beams reached a run-out, 1,000,000 cycles, without failure.
[c] One beam tested at maximum load of 50, 51.5, 52.5, 53, 54 and 55 kN.

in an epoxied groove (using SIKADUR 330) along the bonded length. Three strain gauges were installed in the groove at 80 mm (3.15 in.) spacing in the anchorage length of 200 mm. The 30 mm (1.18 in.) strain gauges were placed on the CFRP sheets used for confinement in the bonded section of the strengthened beam at bar location and at midheight.

The beams were subjected to four point bending. Fig. 2 shows the test setup. Load was applied using a MTS SE controller that controlled a servo-controlled hydraulic actuator. The load was measured using a 155 kN (35 kip) load cell that has an accuracy of 0.1 kN (22.5 lb). The readings of the strain gauges, the LVDTs and the load cell were recorded using a National Instrument SCXI data acquisition system at a sampling rate of 20 readings per second.

Two different types of loading were used: monotonic loading and repeated loading. In the monotonic loading test, the beam was loaded in displacement control at a rate of 1.5 mm (0.06 in.) per minute until the beam failed. The fatigue tests were performed under load control. A sine wave load cycle was applied about the mean load using the MTS 407 controller at a frequency of 2 Hz. The minimum load was set at 10% of the maximum static load capacity of the control beam, so that the beam would not slip or bounce. The maximum load levels were varied to give fatigue lives between 10,000 and 1,000,000 cycles (Table 1). Those fatigue lives were chosen to produce an *S–N* curve covering the fatigue lives of interest to designers.

3. Experimental results

3.1. Static beam tests

Three beam-anchorage specimens were tested in this study under monotonic loading. Beam M-U-100-n and Beam M-R-100-n were both uncorroded, however the former was not strengthened while the latter was strengthened with a U-CFRP sheet. Beam M-U-100-l was corroded to a low corrosion level (3.5%) and not strengthened.

The load versus midspan deflection curve for the three beams tested monotonically showed a linear behaviour up to the maximum load (Fig. 3). Beam M-U-100-n reached a maximum load of 99.7 kN (22.41 kips). The corrosion of the internal steel reinforcement caused a reduction in the maximum static capacity of the beam to 73.7 kN (16.57 kips), i.e. a 25% decrease in comparison with the uncorroded beam. The use of the U-CFRP wraps in the anchorage zone of the uncorroded beam increased the beam's static capacity by 173% compared to the uncorroded, unstrengthened beam. The beam reached 172.7 kN (38.82 kips) maximum load.

A longitudinal crack at the bottom of the beam that initiated at the loaded end of the anchorage zone (next to the pocket) was observed. This longitudinal crack propagated along the length of the anchorage zone. After failure, the bar in the bonded region was removed to inspect the failure which occurred at the bar–concrete interface. It was observed that the concrete above the bar was crushed in some places and intact in others. However the concrete underneath the bar was intact (Fig. 4). This suggests that the concrete above the bar, which was held to the bar by the stirrups, resisted slip and was crushed while the concrete below the bar was split off and pushed away offering little resistance to slip.

3.2. Strain analysis

Three strain gauges were mounted in one of the bars in each beam along the bonded length and a forth gauge in the pocket. Fig. 5 shows the strain variation with load for beam M-R-100-n along the length of the bar starting from the support (0 mm). It is evident that no stress discontinuity has occurred although the bar was un-bonded beyond the pocket location. The increase in the tensile force in the beam beyond this point was taken by the CFRP strips that were added to the sides of the beam. Hence no increase in stress occurred beyond that point (pocket location) and the force in the bar remained constant. Before cracking, it is clear that the strain along the length of the bar in the anchorage zone (200 mm) is linear. As the load increased, cracks appeared in the beam at the anchorage zone level of the bar. These cracks caused a sudden local increase in the strain values of the strain gauges mounted nearest to the cracks. For beam M-R-100-n, the first crack occurred close to strain gauge 3 at a load of about 140 kN, and then at the maximum load (172.7 kN) a crack was observed close to strain gauge 2 accompanied by a sudden increase in gauge 2 strain value (Fig. 5). This strain pattern of sudden increases in strain readings close to cracks was similar for all the monotonic beams. The introduction of the FRP strips on the sides of the beams (away from the anchorage zone) removed the change in the nominal stress in the bar at the end of its un-bonded length; however, there are still stress discontinuities at cracks.

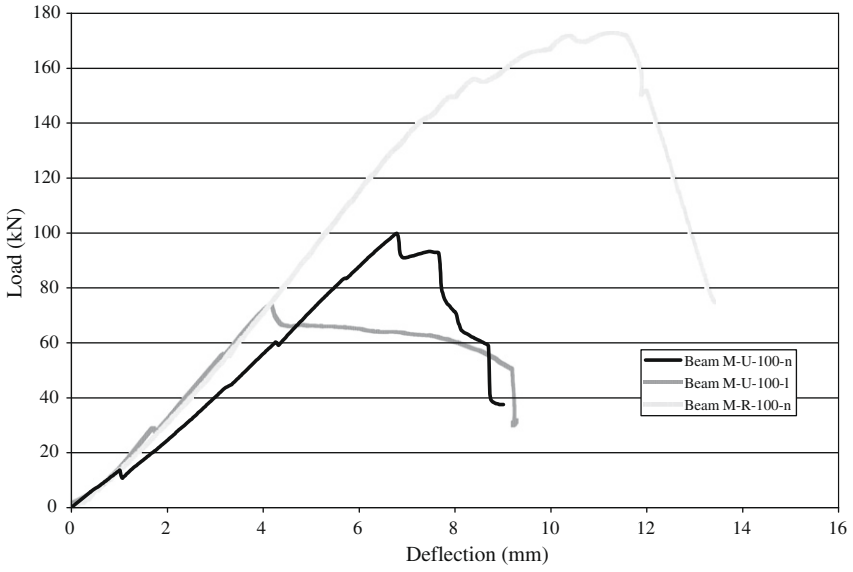

Fig. 3. Load deflection curve for beams tested under static load.

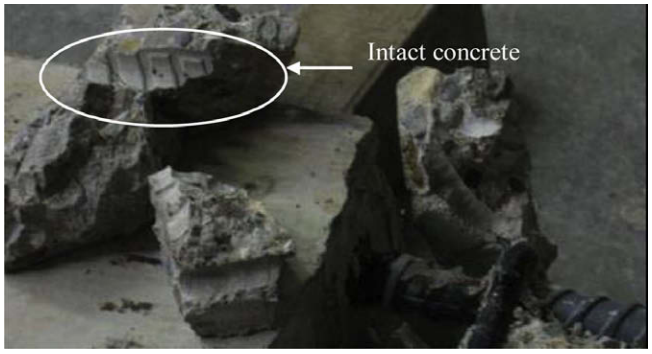

Fig. 4. Intact concrete taken from the anchorage zone from below the steel bar.

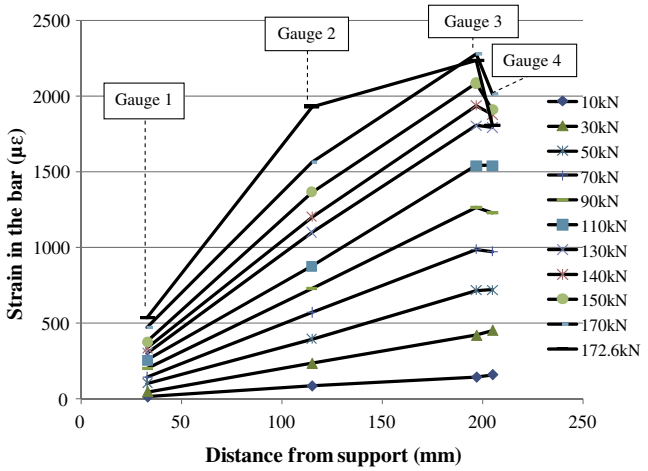

Fig. 5. Strain variation with load along the length of the bar for beam M-R-100-n.

3.3. Bond strength

The average bond stress was calculated as the difference in the force in a bar between two strain gauges divided by the bar surface area between the two strain gauges as given in:

$$u = \frac{A_b f_s}{\pi d_b l} = \frac{f_s d_b}{4l} = \frac{E d_b (\varepsilon_{s2} - \varepsilon_{s1})}{4l} \quad (1)$$

where, u is the average bond strength in MPa, A_b, the cross-sectional area of the steel bar in mm^2, f_s, the steel stress in the bar in MPa, d_b, the bar diameter in mm, ε_{s1} and ε_{s2} are the strain gauge values at locations 1 and 2 respectively along the reinforcement length ($\mu\varepsilon$), l, the length of the bar between two gauges in mm.

The steel stress (f_s) in the bar length at a given strain gauge location was calculated from the strain (ε) measured at that point multiplied by the modulus of elasticity, E, (200,000 MPa [29,007 ksi]) since the bar did not yield.

Fig. 6 shows the average bond stress versus applied load behaviour for both bars in beam M-U-100-n. This behaviour is typical for the static beams. The bars had almost the same bond stress until close to failure when bar 2 had a higher bond stress and slipped causing the beam to fail. For bar 2, the shear stress was found to increase with increasing load up to a maximum shear stress value of 7.68 MPa (1.11 ksi). The strengthened beam had a maximum shear stress of 7.9 MPa (1.15 ksi). The maximum shear stress dropped to 5.6 MPa (0.81 ksi) for the corroded beam M-U-100-l. This decrease is attributed to cracking and concrete crushing around the lugs during corrosion that reduced the bond between the steel and the concrete interface.

3.4. Steel slip behaviour

In the following discussion, the free end refers to the location of the support where the anchorage zone begins. The loaded end is defined as the point close to the pocket where the anchorage zone of the steel reinforcement ends.

Fig. 7 shows the load-slip behaviour of beam M-U-100-n. It can be seen that the slip increased with increasing load at a slow rate until the maximum load was reached after which the slip increased at a much higher rate. Up to the maximum load the slip was higher in the loaded end than the free end. Beyond this point, the opposite was seen with a higher slip at the free end as the load dropped. Initially the longitudinal cracking in the concrete started in the loaded end causing a decrease in the bond between the steel and concrete. Since the concrete in the free end is still uncracked, the slip is small. As the load increases, longitudinal cracking propagates along the anchorage zone causing the bar at the free end to slip at an increasing rate until complete failure of the beam occurs. The beam continued to carry load beyond the maximum load point until a slip of 1.5 mm was reached, then the load dropped abruptly (Fig. 7).

Fig. 8 shows the average bond stress–slip behaviour of the bars in beam M-U-100-n. The shear stress increased with increasing slip until the maximum load was reached. Then the load dropped causing a drop in the shear stress as the slip continued to increase. A similar behaviour was observed for the corroded beam. For the strengthened beam, the shear stress increased with increasing slip until the maximum stress in the bar was reached. Then for a period the shear stress remained constant as the slip and the load continued to increase. The shear stress then decreased at a slow rate with increasing slip until the maximum load was reached when a sudden failure of the beam occurred accompanied by a sudden decrease in the shear stress (Fig. 9). This behaviour is attributed to the fact that after reaching the maximum stress in the bar, the FRP confinement was able to hold the beam together until the maximum load was reached when a sudden failure occurred due to the rupture of the FRP sheet.

3.5. Fatigue beam tests

All of the beams tested under repeated loading were first loaded up to the maximum load manually. The load was then decreased to the mean load, after which the beam was cycled at a frequency of 2 Hz. Table 1 gives a summary of the fatigue lives of the beams tested in the current study.

As the number of cycles increased, a longitudinal crack initiated and propagated at the loaded end of the anchorage zone from the bottom of the beam. This crack continued to increase in length and width until final failure of the beam by bond.

Three uncorroded beams were tested under repeated loading. The minimum load was fixed for all the beams at 10% of the maximum capacity of the control beam (10 kN [2.25 kips]). The first beam was tested at a maximum load of 50 kN (11.24 kips). This beam reached one million cycles with no failure (one million cycles was considered as a run-out for the beams in this study and defined as a one million cycle endurance limit). This beam was then re-tested at a maximum load of 58 kN (13.04 kips), 65 kN (14.61 kips), and 73 kN (16.41 kips). At all these levels the beam reached one million cycles without failure. The beam was then tested at a maximum load of 80 kN (17.98 kips) (load range of 70 kN (15.74 kips)) which resulted in a failure at 4022 cycles. This beam was named F-U-70-n1. Another beam (F-U-70-n2) was tested at a maximum load of 80 kN (17.98 kips) to confirm that the run-out tests the previous beam was exposed to did not cause any noticeable damage. Beam F-U-70-n2 experienced a bond failure at 6524 cycles. These results differ from those reported by

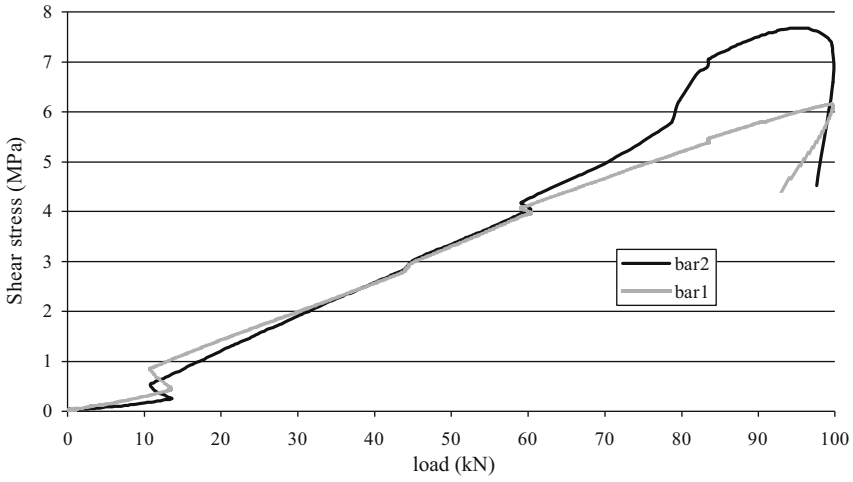

Fig. 6. Shear stress versus load for both bars in beam M-U-100-n.

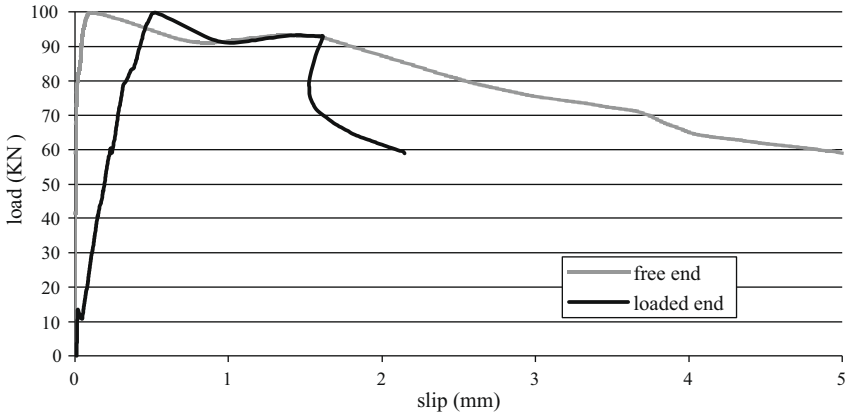

Fig. 7. Load versus slip for bar 2 at the loaded end and free end for beam M-U-100-n.

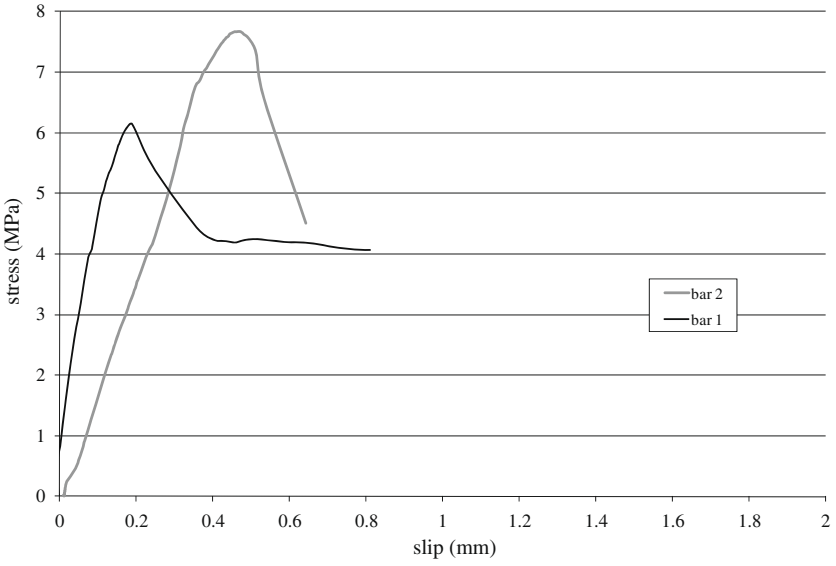

Fig. 8. Shear stress versus slip for both bars in beam M-U-100-n.

[23] where a maximum load of 65 kN (14.61 kips) led to a bond fatigue life of 1714 cycles. Table 1 shows a comparison between the results of [23] and the current study. The major difference between the two studies is that the current study introduced longitudinal CFRP sheets (bonded along the length of the beam beyond the pocket) in order to remove the stress raiser that was present in

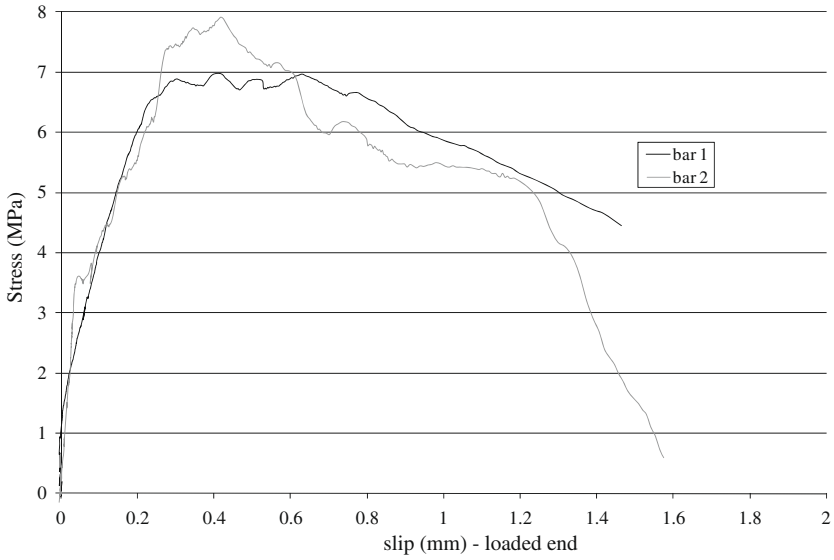

Fig. 9. Shear stress versus slip for both bars in beam M-W-100-n.

the experiments of [23]. Since the bar is un-bonded in the middle, the stress in the bar at midsection will be constant along the whole un-bonded length causing a stress raiser at the beginning of the bonded length of the bar. The introduction of the CFRP sheets reduced the stress in the bar at the middle section of the beam, hence reducing the stress in the bar at the beginning of the bonded length. In addition the current study reduced the effect of confinement from the supports by changing the loading point to the sides of the beam. From the experimental results, it appears that removing the stress raiser significantly increases the nominal bond strength under repeated loading.

After failure of the beams, the failure surface was inspected. It was observed that the bottom concrete of the beam cracked into pieces (Fig. 10a). When these pieces were removed the concrete was found to be intact. The bars were then cut and removed from the beam to inspect the upper concrete to which the bar was held by the stirrups. It was found that the upper concrete between the lugs was partially crushed (Fig. 10b).

The fatigue results for the corroded beams were close to the results that were reported by [23] (Table 1). The removal of the stress raiser in the bar did not have a large effect on the behaviour of these beams. During an examination of the contact surface at failure, it was noticed that the concrete in between the lugs was already partially crushed due to the rust product from the corrosion process (Fig. 11). This reduced the strength of the concrete keys and increased the rate of slip in the bar under repeated loading.

3.6. Fatigue strength

The fatigue life of the tested beams was plotted versus the applied load range in Fig. 12. The data for the fatigue strength was represented by a curve obtained by plotting a best fit line through the experimental fatigue life data. It can be noted that the fatigue life of the beams varies linearly with the applied load range with a very shallow slope on the logarithmic scale. Hence the range over which fatigue failure occurs is very small. Corroding the beams to a low (3.9%) corrosion level decreased the fatigue strength by about 30%. This decrease did not vary significantly with fatigue life. Corrosion leads to the formation of rust products that are greater in volume than the steel bar itself. These rust products cause stresses in the concrete leading to crushing of the concrete keys at the steel to concrete interface during corrosion. This crushing decreases the fatigue bond strength and therefore causes a reduction on the fatigue strength of the beam. The forces causing this crushing also caused longitudinal surface cracks in the beams at the reinforcement level.

3.7. Strain variation for fatigue beams

The readings from the strain gauges mounted on the steel bar were plotted versus their locations on the bar for various percentages of the fatigue life of a beam. Fig. 13 shows the strain variation along the length of the steel bar for beam F-U-70-n2 starting from the support (0 mm). The strain increased linearly with distance

Fig. 10. (a) The cracks after failure in the bonded region of beam F80-U-n1 turned upside down. (b) Intact concrete in the top bar of the beam in beam F80-U-n2.

Fig. 11. Fattigue failure in beam F-U-43-l: (a) upper concrete above bar and (b) lower concrete below the bar.

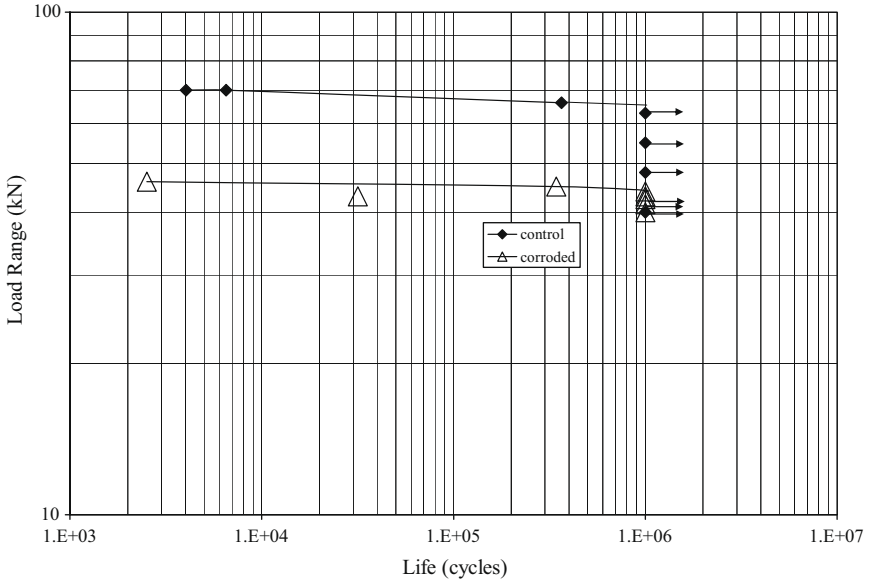

Fig. 12. Variation in load range with life for beams failing in fatigue of bond.

from the support. The last data point in each plot is the strain in the bar mounted at the pocket. It is clear from the strain readings that due to the introduction of the FRP strips on the sides of the beam there is no discontinuity in the strain along the bar between the bonded region and the un-bonded region (Fig. 15). The small variation in the readings of the strain gauges mounted at the pocket (un-bonded region) is probably due the inaccuracy in the FRP strip width, which will cause a slightly higher or lower strain value. The strain values increase with the increase in the number of cycles. As local cracks appear, the local strains show a sudden increase. At 100% of the fatigue life, a horizontal crack ran between the locations of strain gauges 2 and 3 as part of the concrete debonded along the bar between these two points (dashed line in Fig. 13). There was a reduction in the strain reading at point 3 that can probably be attributed to a reduction in the bar force as the central cracks opened, the neutral axis moved up, and the distance between the centroid of the concrete force and the steel bar increased.

3.8. Fatigue shear stress

The average bond stress at the maximum load was calculated using Eq. (1). The nominal shear stress was almost constant along the anchorage length of the bar, unlike the tests of [22] in which the nominal shear stress was much higher at the loaded end than at the free end. This was due to the presence of the CFRP sheets along the sides of the beam in the un-bonded region that maintained the curvature constant along the length of the bar beyond the end of the anchorage zone. This shear stress did not change with the number of cycles until failure when the shear stresses decreased due to bond failure (Fig. 14). This behaviour was typical for both uncorroded and corroded beams. However for the corroded beams, the shear stress was smaller than for the uncorroded beams. The shear stress was between 2.5 and 3.5 MPa (362.6 and 507.6 psi) for the corroded beams, while it varied between 4.5 and 5.5 MPa (652.7 and 797.7 psi) for the uncorroded beams.

3.9. Steel slip behaviour

Slip was measured as the relative movement between the steel bar and the concrete. The steel slip was measured using LVDT's that were mounted on the steel bar at the free end (end of beam) and the loaded end (in the pocket). The measured slip at the loaded and the free ends for bars 1 and 2 was almost the same. The slip remained almost constant as the number of cycles increased until failure when the slip increased suddenly (Fig. 15). In the control

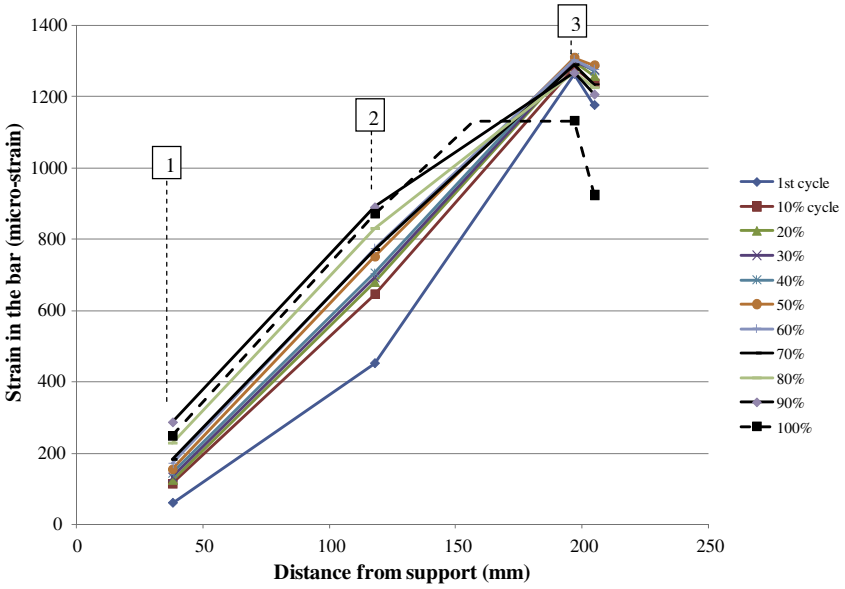

Fig. 13. Strain variation with respect to percentage of fatigue life along the distance of the bar for Beam F-U-70-n2.

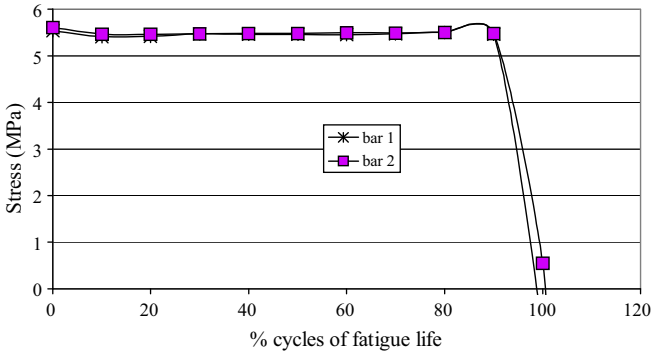

Fig. 14. Stress versus cycles for both bars in beam F-U-70-n1.

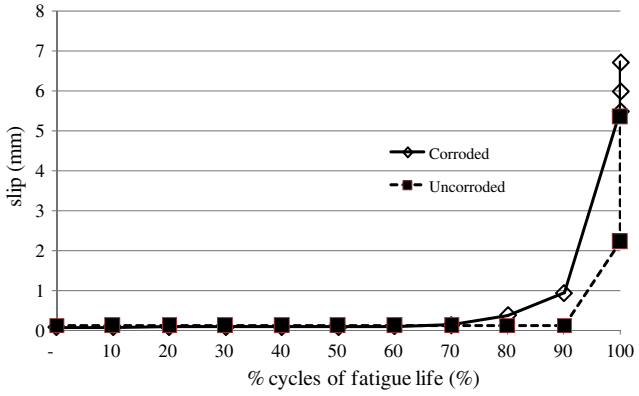

Fig. 15. Typical slip behaviour of the bars with respect to the number of cycles (corroded: beam F-U-43-l; uncorroded: beam F-U-70-n1).

uncorroded beams there was not much increase in slip with cycles until failure occurred. On the other hand, the corroded beams showed an increase in slip earlier in the fatigue life (Fig. 15).

4. Conclusions

The bond behaviour of corrosion damaged reinforced concrete beams was investigated under monotonic and repeated loading. The beams subjected to repeated loading were cycled at a frequency of 2 Hz with a load range varying between 40 and 70 kN in order to achieve fatigue lives representative of service conditions (between 1000 and 1000,000 cycles). The following are the main conclusions of the study:

- Corroding the reinforcing steel in the beams to a low corrosion level (3.9%)reduced their maximum static capacity by 25% and their fatigue strength by about 30%.
- Corroding the reinforcing steel in the beams formed rust products that caused the concrete in between the lugs to crush, reducing the strength of the concrete keys and increasing the rate of slip in the bar under repeated loading. Strengthening the beam with a transverse U-shaped CFRP sheet in the anchorage zone increased the static capacity of the beam by 173%.
- The introduction of the CFRP longitudinal strips on the sides of the beam beyond the bonded length of the bar resulted in a zero nominal shear stress along the un-bonded region of the beam.
- Examining the concrete around the bar after failure, it was noticed that the concrete above the bar, which was held to the bar by the stirrups, resisted slipping and was crushed while the concrete below the bar was split off and pushed away offering little resistance to slip.
- The fatigue life of the beams varies linearly with the range of load applied with a very shallow slope.
- Comparing the fatigue results of the current study to the study presented by [23], it is clear that the stress raiser introduced at the end of the anchorage zone in the previous study reduced the fatigue lives of the uncorroded beams.

Acknowledgments

The authors would like to acknowledge support received from NSERC and the ISIS Canada Network of Centers of Excellence. The donation of the CFRP sheets from SIKA Canada and the concrete from Hogg Ready Mix is appreciated. The help in laboratory work provided by the University of Waterloo technicians and the other members of the rehabilitation research group at the University of Waterloo is greatly appreciated.

References

[1] Broomfield JP. Corrosion of steel in concrete: understanding, investigation and repair. London: E&FN Spon; 1997.

[2] ACI Committee 222. Protection of metals in concrete against corrosion (ACI 222-01). Farmington Hills (MI): American Concrete Institute; 2001.

[3] Zhang JY, Mailvaganam NP. Corrosion characteristics and key electrochemical factors in patch repair. Can J Civ Eng 2006;33(6):785–93.

[4] ACI Committee 408. Bond and development of straight reinforcing bars in tension (ACI 408R-03). Farmington Hills (MI): American Concrete Institute; 2003.

[5] Fédération Internationale du Béton (fib). Bond of reinforcement in concrete, state-of-art report. In: International federation for structural concrete, Switzerland; 2000.

[6] Al-Sulaimani GJ, Kaleemullah M, Basunbul IA, Rasheeduzzafar. Influence of corrosion and cracking on bond behaviour and strength of reinforced concrete members. ACI Struct J 1990;87(2):220–31.

[7] Cabrera JG, Ghodoussi P. The effect of reinforcement corrosion on the strength of the steel/concrete bond. In: Riga Latvia, editor. Proceedings: bond in concrete – from research to practice; 1992. p. 10.11–24.

[8] Clark LA, Saifullah M. Effect of corrosion on reinforcement bond strength. In: Proceedings of the fifth international conference on structural faults and repair. UK: University of Edinburgh; 1993. p. 113–9.

[9] Rodriguez J, Ortega L, Casal J. Corrosion of reinforcement bars and service life of reinforced concrete structures: corrosion and bond deterioration. In: Proceedings: concrete across borders, Odense, Denmark, vol. 2; 1994. p. 315–26.

[10] Almusallam AA, Al-Gahtani AS, Aziz A, Rasheeduzzafar. Effect of reinforcement corrosion on bond strength. Constr Build Mater 1996;10(2):123–9.

[11] Mangant PS, Elgarf MS. Bond characteristics of corroding reinforcement in concrete beams. Mater Struct 1999;32(2):89–97.

[12] Auyeung Y, Chung L, Balaguru P. Bond behaviour of corroded reinforced bars. ACI Mater J 2000;97(2):214–20.

[13] Fang C, Lundgren K, Chen L, Zhu C. Corrosion influence on bond in reinforced concrete. Cem Concr Res 2004;34(11):2159–67.

[14] ACI Committee 215. Considerations for design of concrete structures subjected to fatigue loading. Farmington Hills (MI): American Concrete Institute; 1997.

[15] Mor A, Gerwick BC, Hester WT. Fatigue of high-strength reinforced concrete. ACI Mater J 1992;89(2):197–207.

[16] ACI Committee 408. State-of-the-art report on bond under cyclic loads (ACI 408.2R-92). Farmington Hills (MI): American Concrete Institute; 1992.

[17] Al-Hammoud R. Fatigue flexural behaviour of corroded reinforced concrete beams repaired with CFRP sheets. MSc thesis. Waterloo, Ontario: University of Waterloo; 2006.

[18] Masoud S, Soudki K, Topper T. Postrepair fatigue performance of FRP-repaired corroded RC beams: experimental and analytical investigation. ASCE J Compos Construct 2005;9(5):441–9.

[19] ACI Committee 440. Report on fibre-reinforced polymer (FRP) reinforcement for concrete structures (440R-07). Farmington Hills (MI): American Concrete Institute; 2007.

[20] El Maaddawy T, Soudki K. Effectiveness of impressed current technique to simulate corrosion of steel reinforcement in concrete. ASCE J Mater Civ Eng 2003;15(1):41–7.

[21] ASTM Standard G1-03. Standard practice for preparing, cleaning, and evaluating corrosion test specimens V. 03.02.. Annual Book of ASTM Standards; 2003. p. 17–25..

[22] ACI Committee 440. Design and construction of externally bonded FRP systems for strengthening concrete structures (440.2R-08). Farmington Hills (MI): American Concrete Institute; 2008.

[23] Rteil AA. Fatigue bond behaviour of corroded reinforcement and CFRP confined concrete. PhD thesis, Waterloo (Ontario): University of Waterloo; 2006.